Impact of Wi-Fi interference on NavIC signal

Darshna D. Jagiwala* and Shweta N. Shah

Electronics Engineering Department, Sardar Vallabhbhai National Institute of Technology, Surat 395 007, India

The Navigation with Indian Constellation (NavIC) designed by the Indian Space Research Organisation (ISRO) is an autonomous regional satellite navigation system for providing accurate real-time positioning and timing services to India up to 1500 km from its boundary. The NavIC system exploits L5- and S-band for its navigation. The performance of these bands may be interfered by other bands or out-of-band communication systems, which can be the main threat to the performance of the NavIC receiver. This article focuses on real-time out-of-band interference of Wi-Fi signals in the S-band of the NavIC receiver. The performance analysis is carried out with respect to power spectral density, histograms, execution of acquisition stage and parameters of hypothesis testing method like *P*-value, confidence interval to identify the presence of interference on the NavIC receiver. All these results show that the Wi-Fi signal transmission represents a potential source of interference for NavIC applications and causes severe degradation on NavIC satellite signals.

Keywords: Power spectral density, radio frequency interference, satellite navigation system, Wi-Fi signals.

THE satellite navigation system contributes to autonomous geo-spatial positioning with regional or global coverage. To find the location of any user in the form of longitude, latitude and altitude, satellites transmit the Line-of-Sight (LOS) signals from space. One of the main challenges of any Global Navigation Satellite System (GNSS) signal is the low-level signal power to the receiving antenna. Thus, weak signals at the GNSS receiver after travelling from the space station to earth are prone to radio frequency interference (RFI)[1]. The Navigation with Indian Constellation (NavIC) receiver is a dual-frequency band receiver operated on L5 (1176.45 MHz) and S-band (2492.08 MHz) frequencies. Many communication services coexist in the same band due to the limitation of the frequency spectrum. The frequency of L5-band is globally allocated to the Aeronautical Radio Navigation Service (ARNS), which is also shared by other navigation systems like NavIC L5, Global Positioning System (GPS) L5 and Galileo E5 (refs 1, 2). Moreover, S-band is utilized by NavIC only if navigation systems are considered, but this band is shared by other communication systems like Long-Term Evolution (LTE), Bluetooth, Wireless Fidelity (Wi-Fi/IEEE 802.11 standard) and Industrial Scientific Medical (ISM) band (Figure 1)[3]. The strengths, weaknesses and applications of navigation in S-band are briefly described in the literature[4,5]. Currently, the usage of LTE devices is increasing exponentially. In this situation where Wi-Fi receivers are present in every cell phone, the study of Wi-Fi interference is necessary to verify the performance of NavIC signal reception. This kind of interfering signal represents a threat to the performance of the satellite receiver by which accuracy, availability, stability and reliability of the navigation service may be affected.

In order to make the receiver less susceptible to RFI, the interference should be detected and mitigated either before the correlation (pre-correlation detection) or after it (post-correlation detection)[1,2]. In pre-correlation techniques, antennas, IF signal processing, values of automatic gain control (AGC) and analog to digital converter (ADC) have been used to detect RFI, and in post-correlation techniques, the carrier-to-noise ratio (C/N_0), position, velocity and time (PVT) of the input signal affected by RFI are normally used to identify an interference[6]. The pre-correlation techniques are more efficient and faster than post-correlation techniques for interference detection and mitigation.

Interference mitigation techniques can be clustered in time, frequency, time–frequency, and timescale domains, according to the nature of interference[1,2]. In the time domain, pulse blanking technique is the most popular, targeting the excision of pulsed interference (e.g. DME/TACAN). The frequency domain mitigation techniques are generally used to remove the harmonic components of an interfering signal from the composite received signal spectrum. In the time–frequency domain, ADC samples are employed in order to perform the time–frequency representation of an incoming interfered signal. Each value

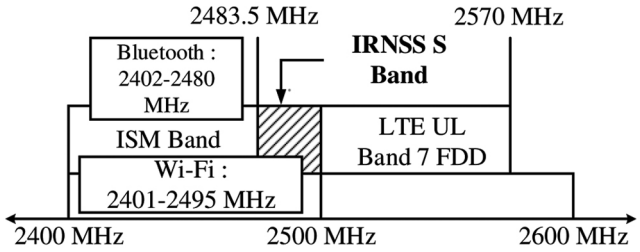

Figure 1. Use of spectrum in S-band[3].

*For correspondence. (e-mail: darshna12@gmail.com)

in the transformed domain is compared to a mask, which is computed through an orthogonal-like Gabor expansion on the expected GNSS received signal that would be present in an interference-free environment. To obtain time-scale representation of the incoming interfered signal, wavelet transform has been recently employed[1].

This article focuses on the interference detection approach. The pre-correlation detection method is implemented in two stages[7]. In the first stage, an interference-free window of data is treated in order to obtain a threshold for narrow-band interference. In the second stage, a two-sample *t*-test is performed on the sample mean of the time series to reveal the existence of anomalies. A similar technique was proposed by Balaei and Dempster[8] in the frequency domain for narrow-band interference. Both time and frequency domain detection methods have been analysed by Tani and Fantacci[9] and the use of spectral Welch estimation approach was proposed as an interference detection algorithm for narrow-band frequency modulation (FM) interference. In this study, hypothesis testing is analysed to verify the existence of Wi-Fi interference on NavIC signal. An assessment window (without RFI) of data and an evaluation window (with RFI) are first divided into blocks and then analysed to obtain the hypothesis parameters as given in Marti and van Graas[7].

Mathematical modelling of hypothesis testing

Hypothesis testing is a standard way to draw inferences about a population based on statistical evidence from a sample. Here, the existence of interference is identified based on two-sample *t*-test method of hypothesis testing. As shown in Figure 2, the population 1 is from a part of the NavIC signal which is without RFI, referred as the assessment window and the population 2 is a part of the NavIC signal with RFI to be tested and is considered as an evaluation window. Each window is then divided into a number of data blocks (DB) which have the number of sample size (SS). The size of the assessment and evaluation windows is assumed to be equal to the window size (WS), as presented in Figure 3. So WS = SS × DB. The size of WS, SS and DB is related to the sampling rate of the front end of the receiver.

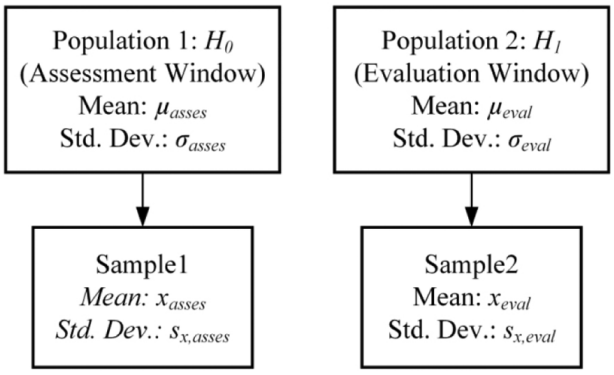

Figure 2. Independent sampling from two populations.

The objective of hypothesis testing is to use the information in the samples to estimate the difference $\mu_{\text{asses}} - \mu_{\text{eval}}$ in the means of the two populations, and make statistically valid inferences about it. The central limit theorem (CLT) permits the use of this method for large samples, even when the two populations of interest are not normal[8]. The following steps are performed to check the presence of interference by observing the behaviour of parameters like *P*-value and confidence of interval (CI) between these two populations[7–10].

Step 1: Define null and alternative hypothesis. Consider the absence of an interference signal hypothesis H_0 (null hypothesis) and presence of interference signal hypothesis H_1 (alternative hypothesis). Here H_0 and H_1 are complementary hypotheses. In this article, based on statistical inference of the assessment and evaluation windows, the hypothesis test has been introduced to verify the differences between the population samples of the assessment and evaluation windows. Thus, the null hypothesis is defined as

$$H_0 = x_{\text{eval}} - x_{\text{asses}} = x_d = 0. \tag{1}$$

The alternative hypothesis is defined as

$$H_1 = x_{\text{eval}} - x_{\text{asses}} = x_d \neq 0, \tag{2}$$

where x_{eval} and x_{asses} are the sample means of the evaluation and assessment windows respectively, and x_d is the difference between these two sample means.

Step 2: Calculate the test statistic of the assessment and evaluation windows.

The test-statistic can be obtained as follows[8]

$$T(N-1) \cong \frac{x_{\text{asses}} - x_{\text{eval}}}{\sqrt{(S^2_{x,\text{asses}} + S^2_{x,\text{eval}})}}, \tag{3}$$

where $S^2_{x,\text{asses}}$ and $S^2_{x,\text{eval}}$ are the samples standard deviations of the assessment and evaluation windows respectively.

Step 3: Calculate the *P*-value of the test static. The *P*-value is the probability of the test statistic which is calculated under the assumption that the null hypothesis is true. Two types of errors can occur in making this decision. Type-I error is the rejection of a true null hypothesis and type-II error occurs when the null hypothesis is accepted and the alternative hypothesis is the true state of nature. The significance level, denoted by α, is the probability of making a type-I error: that of rejecting a null

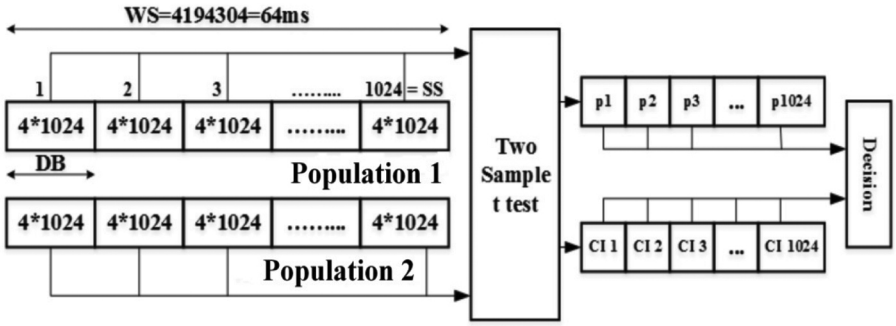

Figure 3. Process of hypothesis testing.

hypothesis which is, in reality, true. If the *P*-value is less than or equal to α, then reject H_0. If the *P*-value is greater than α, fail to reject H_0.

Step 4: Calculate the confidence interval. It is this region (or interval) of test-statistic values that would lead to the acceptance of H_0. Test-statistic values that fall outside of this interval would lead to a rejection of H_0 and an acceptance of H_1. A 95% CI returns a significance level of 0.05. If it is hypothesized that a true parameter value is zero, but the 95% confidence interval does not include zero, then the estimate is significantly different from zero at the 5% significance level. Hence 100 $(1 - \alpha)$% CI for the difference between two population means can be calculated as follows

$$(x_{\text{asses}} - x_{\text{eval}}) \pm t_{\alpha/2} \sqrt{\left(\frac{S^2_{x,\text{asses}}}{n_1} + \frac{S^2_{x,\text{eval}}}{n_2} \right)}. \quad (4)$$

In eq. (4), $t_{\alpha/2}$ is the value for which the distribution *T* with $N - 1$ degrees of freedom has a tail probability equal to $\alpha/2$. Thus, if the range of CI defined in eq. (4) does not include zero, it indicates that the presence of interference on the useful signal is accepted.

Experimental set-up

This section focuses on the methodology used to observe the effects of the Wi-Fi signal as a threat to S-band of the NavIC receiver. In this study, digitized IF samples of the NavIC signal have been collected using the Accord NavIC User Receiver (NavIC-UR) at the Communication Research Lab of the Electronics and Communication Engineering Department, SVNIT, Surat (21 : 16° lat., 72 : 78° long.)[11,12]. With the NavIC-UR set-up, a GUI is provided by ISRO which is a Windows-based real-time user interface. The signal strength chart is given in the GUI, which indicates the strength of the received signal in terms of C/N_0. The TP-Link router (model number TL-WA5210G 2.4 GHz) is used as an interfere to the NavIC receiver. Figure 4 *a* and *b* shows the experimental set-up. This experiment is done only for a fixed distance between the NavIC antenna and Wi-Fi router with availability scenario. Table 1 summarizes the parameters of NavIC-UR and Wi-Fi router.

Simulation results and discussion

The real-time digital IF data (without and with interference) have been logged from the front end of the NavIC receiver and simulated for further performance analysis. This experiment has been repeated and the same behaviour of RFI obtained. To identify the presence of interference, various measuring parameters like power spectral density (PSD), histograms, hypothesis testing method have been used. This is to justify the existence of Wi-Fi interference on the real-time data received from the NavIC receiver. The execution is done in MATLAB 2014a. Considering the specifications as given in Table 1 and constant parameters, the S-band signals are analysed without and with interference as case I and case II respectively.

The Orthogonal Frequency Division Multiplexing (OFDM) divides a given channel into many narrow subcarriers. In Wi-Fi OFDM channelization, each 20 MHz channel, whether or not it is 802.11a/g/n/Ac, is composed of 64 subcarriers spaced 312.5 kHz apart; this becomes problematic when other nearby devices are also using the same frequency. When the frequency channel of Wi-Fi overlaps with the frequency of the S-band signal to the NavIC receiver, the effect of interference is observed in the S-band signal of the NavIC receiver due to the extremely low power level of the signal at the user's receiver. This type of interference does not persist in nature, but it depends on the timing and frequency of Wi-Fi, which is as close to the NavIC S-band frequency. Figure 5 *a* and *b* shows the impact of interference for two different situations belonging to the same time duration of this experiment.

The C/N_0 values of S-band signal are degraded from their normal values and the colour of the signal strength turns from blue to red (Figure 5 *a*). If the frequency of the Wi-Fi channel switches close to 2483.50 MHz, severe degradation takes place (Figure 5 *b*) on the S-band signal

of the NavIC receiver. Due to this phenomenon, signal strength of the S-band becomes zero. It shows that the effect of interference/strong out-of-band signals could be more severe, leading to loss of lock and a reduced number of satellites in view.

There is a one-to-one correspondence between signal strength and C/N_0 values. The value of C/N_0 (dB-Hz) of the NavIC S-band signal is affected by Wi-Fi interference. For the particular day and time duration when the experiment was carried out, the graphs of all satellites were generated using the NavIC Data Analysis Software (IRDAS) version 3.0 (provided by ISRO) (Figure 6 *a*). Here C/N_0 values are taken from the logged data of NavIC receiver and graphs of all satellites are plotted using MATLAB considering the specific time of interference. It can be seen from Figure 6 *b* that for this exact duration only, the C/N_0 values are reduced.

To observe the spectrum of the router, one open-ended cable is attached with Agilent spectrum analyzer N9000A. The complete spectrum of the router is shown in Figure 7 *a* and *b* with a peak table which provides information on frequency and power. From Figure 7 *b* it can be clearly observed that the upper frequency band of channel 13 of Wi-Fi is 2483 MHz, but its spurious emission is beyond this frequency which is responsible for interference on S-band of the NavIC receiver. The other simulated results are as follows.

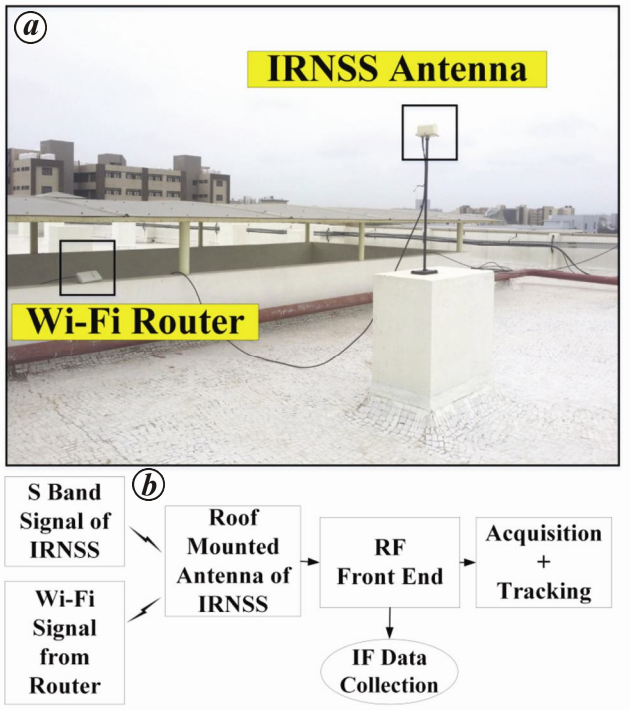

Figure 4. Experimental set-up: ***a***, real time; ***b***, practical.

Table 1. Specifications of NavIC-UR and Wi-Fi router

Parameters of NavIC-UR	Value
Frequency of S-band	2492.028 ± 8.25 MHz
IF frequency	72.221 MHz
Sampling frequency	56 MHz
Bits/sample	4
Antenna polarization	RHCP
LNA gain	>20 dB@S-band
LNA noise figure	<2 dB
Parameters of Wi-Fi router	**Value**
Frequency of channel 13	2472 ± 11 MHz
Power	–19 dBm (approx.)
Maximum data rate	54 Mbps
Modulation	OFDM

Analysis of power spectral density

As a first phase of investigation, the PSD of the IF data is analysed. Figure 8 shows comparison of PSD for case I and case II. In the Bartlett algorithm, the input signal is distributed to M windows that do not overlap, and the length of each window is P. The periodogram is calculated for each window and by averaging the periodograms for the consecutive windows; the Welch power spectrum

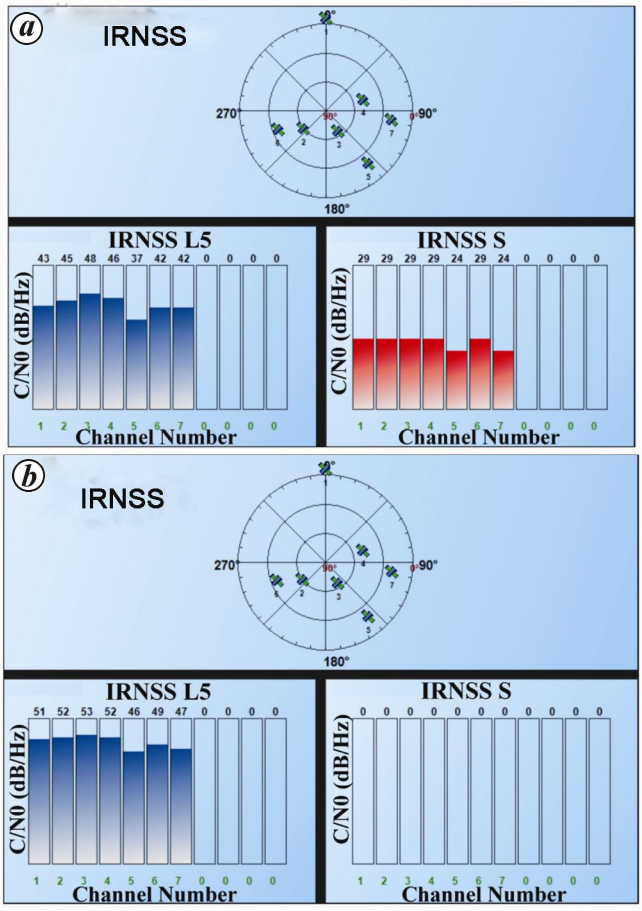

Figure 5. Snapshots of S-band C/N_0 from NavIC receiver GUI[11]. ***a***, Degraded values of C/N_0 due to Wi-Fi interference. ***b***, Zero values of C/N_0 due to severe Wi-Fi interference.

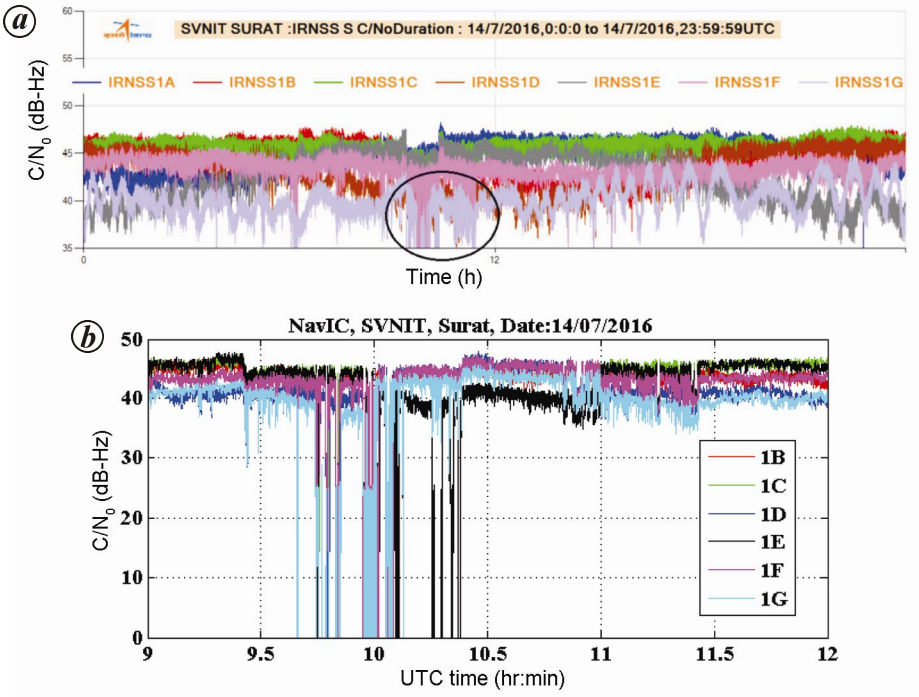

Figure 6. ***a***, Performance of C/N_0 for seven satellites using NavIC data analysis software (IRDAS) version 3.0; ***b***, Simulated result of C/N_0 for six satellites of NavIC at the time of experiment.

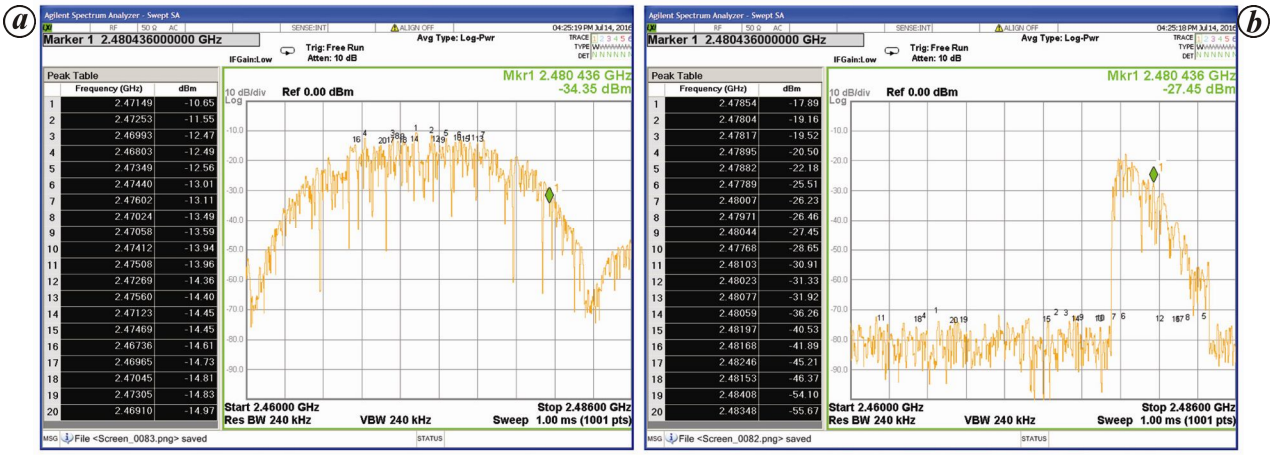

Figure 7. Spectrum of Wi-Fi signal on spectrum analyzer. ***a***, Complete spectrum of Wi-Fi; ***b***, Side band spectrum of Wi-Fi.

is obtained. For the N-point sequence $X(n)$, the method can be presented as[13]

$$\gamma(k) = \frac{1}{N}\sum_{i=0}^{M-1}\left|\sum_{n=0}^{P-1} X_i(n)\exp\left[-j\frac{2\Pi nk}{P}\right]\right|^2, \quad (5)$$

where k is the FFT index and

$$X_i(n) = X(i \times P + n),\ i = 0,\ 1,\ 2,..., M-1. \quad (6)$$

Note that in case II, the amplitude of the spectrum is reduced by 3 dB with respect to the centre frequency and many frequency peaks are found due to interference by the spurious emission of Wi-Fi router. Figure 8 shows that lower frequencies of the S-band signal are affected more compared to a higher range of frequency in case II.

Analysis of histograms

Figure 9 *a* shows the variation in the value of AGC, whether it will increase or decrease to maintain the dynamic range of ADC for proper output[14]. Due to the fact that without RFI, data are overridden by thermal Gaussian noise, the observed distribution of ADC bins is also Gaussian shaped. If the histogram of digital data resembles the one to its right in Figure 9 *a*, then the gain

is found to decrease, and if it resembles the one on its left, then the gain increases until it has the shape of the middle histogram. This result is similar to our simulated result on the NavIC receiver (Figure 9 *b*). It justifies the Gaussian shape of the histogram in the presence and absence of RFI. Here the value of AGC is changed to maintain proper operation of ADC in the presence of RFI. From Figure 9 *b*, it is clearly observed that the strong effect of Wi-Fi interference is present in ADC samples.

Analysis of correlation power at acquisition stage

The first digital signal processing stage of the NavIC receiver is an acquisition block that must determine the presence of the signal and provide an approximate estimate of the input signal[12]. The main operation performed by the acquisition block is to correlate the input signal. The main action accomplished by the acquisition block is to correlate the input signal with local replicas of the signal code and carrier. If the NavIC signal is present in the absence of interference, a single dominant peak should appear in the performance evaluation of the cross-correlation process. The peak reveals the presence of the signal and it is located close to the sampling frequency (F_s). Figure 10 *a* and *b* compares the cross correlation power for case I and case II respectively. In Figure 10 *b*, many peaks appear due to interference of Wi-Fi signal.

Analysis of hypothesis testing

For the purpose of simulation, the null hypothesis (H_0) and the alternative hypothesis (H_1) are considered as defined in eqs (1) and (2) respectively, to evaluate the difference between two sample means using a two-sample *t*-test. Figure 3 shows the complete process of hypothesis testing.

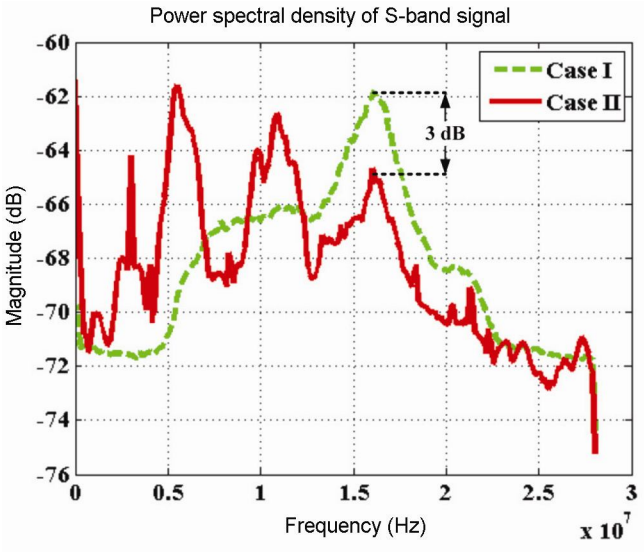

Figure 8. Performance comparison of power spectral density.

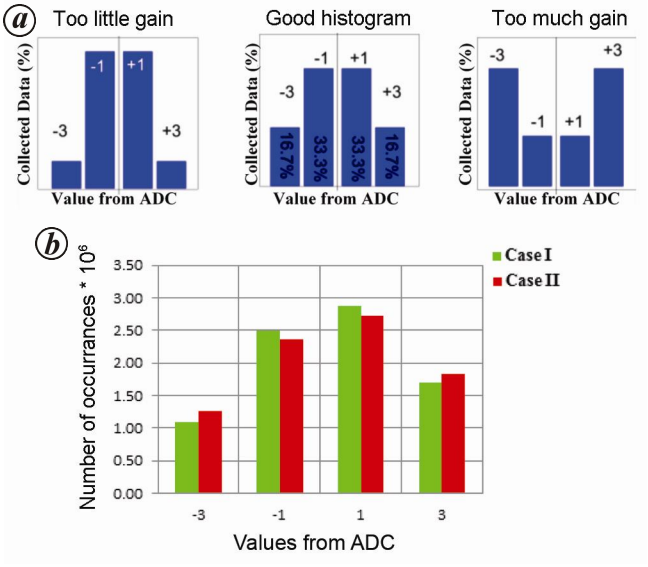

Figure 9. Performance comparison of histograms: ***a***, histogram of GPS signal 14; ***b***, histogram of NavIC signal.

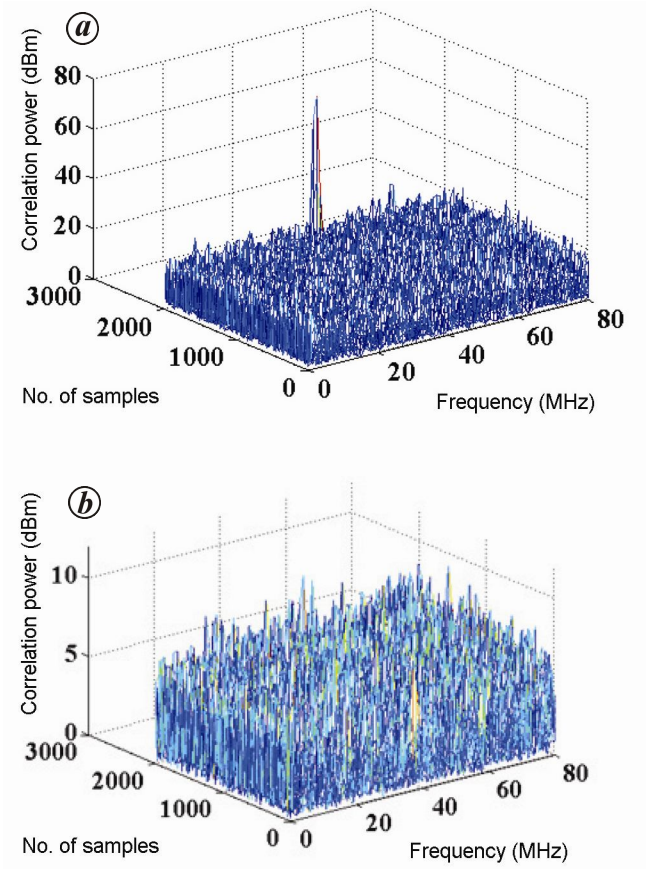

Figure 10. Performance comparisons at acquisition stage: ***a***, Cross correlation power for case I; ***b***, cross correlation power for case II.

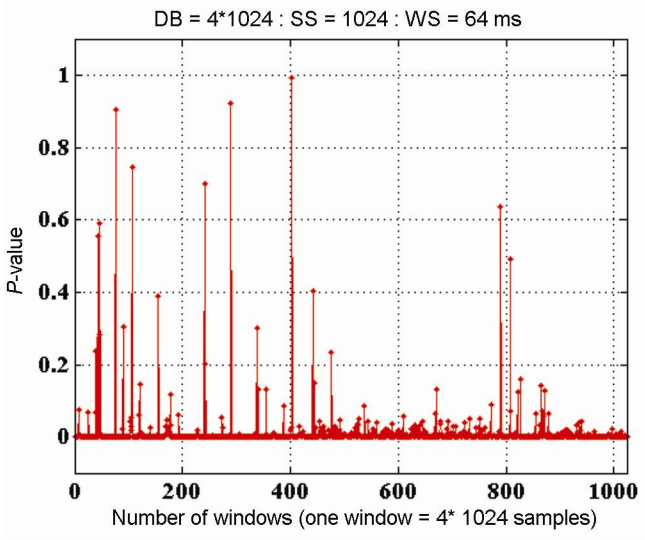

Figure 11. Performance of *P*-value of hypothesis testing.

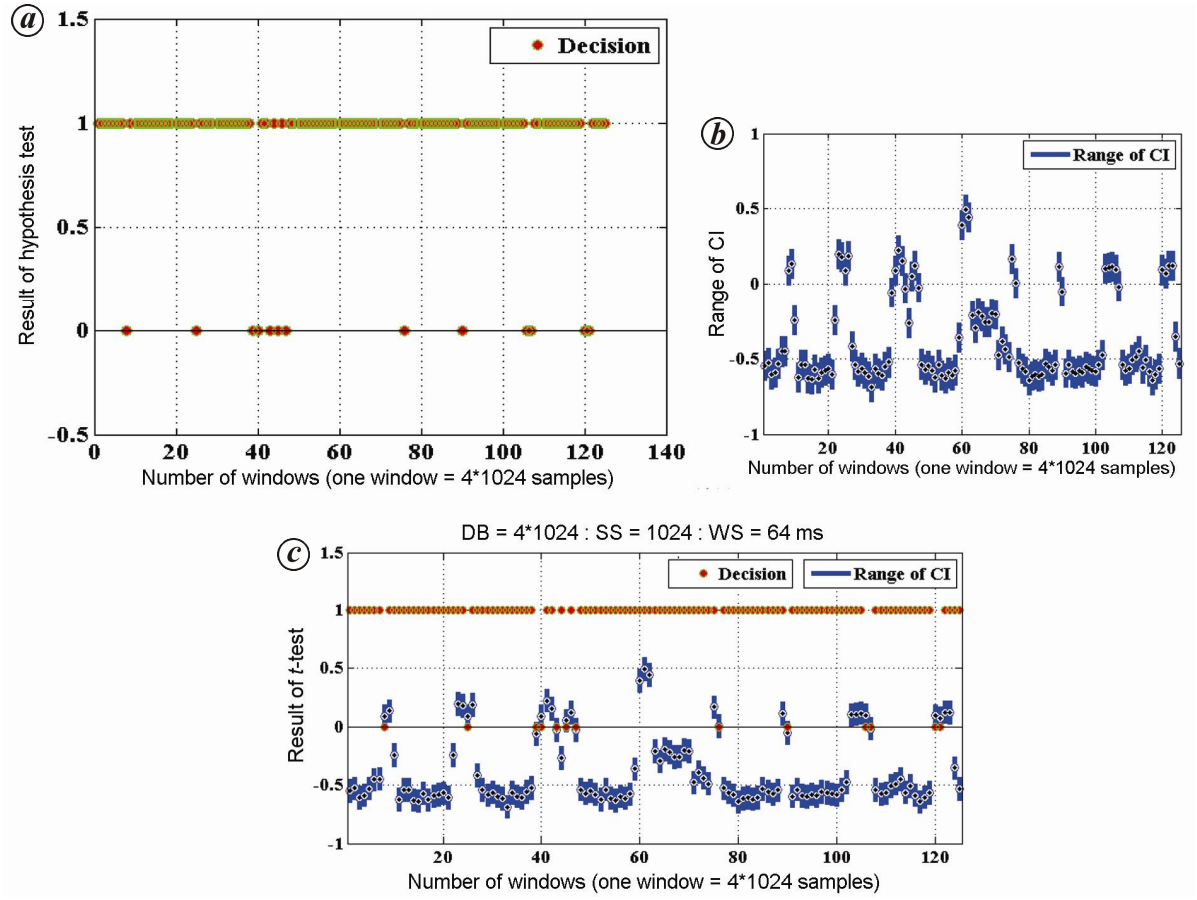

Figure 12. Performance of hypothesis testing: ***a***, decision of hypothesis test; ***b***, range of CI; ***c***, combined graph of decision and range of CI.

The *P*-value of the test gives a measure of how much evidence one can have against the null hypothesis. If the *P*-value from two-sample *t*-test is smaller than the value of α, there is evidence for the existence of interference[8]. The sampling frequency of NavIC is 56 MHz. So the number of samples according to WS = 64 ms is calculated as ($56 \times 10^6 \times 64 \times 10^{-3} = 3{,}584{,}000$). For a better analysis, the number of samples is considered in the form of power of 2. So, a total of 4,194,304 ($\cong 2^{22}$) samples are taken for simulation purpose. The sample window is taken

as DB = 4*1024 as shown in Figure 3. Hence a total of 1024 windows are analysed to observe the performance of hypothesis testing. There is always a trade-off between the sample complexity and computational complexity in signal processing. Hypothesis testing can be done using the WS of 32 ms and 128 ms. To reduce the computational complexity, 64 ms is considered in this study.

The results of the test are follows:

- For each window, *P*-value is calculated. Figure 11 shows the behaviour characteristic of *P*-value. It can be clearly seen that *P*-value of the test, returned as a scalar value in the range [0, 1], can be easily compared with the value of $\alpha = 0.05$ to identify the existence of RFI in each window[10]. If the *P*-value is less than 0.05, the null hypothesis is rejected at the default level $\alpha = 0.05$ and there is interference in that particular window.
- Figure 12 shows the performance of decision and CI. It is difficult to interpret the result of hypothesis testing with 1024 samples. The decision of the test and range of CI cannot be accurately visualized. The response of the results is the same for 1024 and 125 number of samples. The behaviour essentially depends on the existence of an interfering signal. For a better understanding, only 125 samples are considered in the figure. In Figure 12 *a*, the decision of the hypothesis test is shown in Figure 12 *b*, box plot of CI is presented and a combined analysis is shown in Figure 12 *c*. When a range of CI for comparing two populations includes zero, it is possible that there is no difference in their means. Therefore, both hypotheses are equal and interference does not exist in that particular window. According to that, the decision is taken either the null hypothesis is accepted or rejected. From Figure 12 *c*, it is perceived that when CI includes zero at the same time, H_0 becomes zero indicating hypothesis is accepted and there is no RFI for that particular window and vice versa.

Conclusion

Many telecommunications and electronic systems such as mobile satellite networks, FM/TV transmitter harmonics, personal electronics, ultra wideband radar, etc. can interfere with the NavIC reception band of L5 and S. The applications of NavIC such as precision agriculture, marine, aeronautical, timing and synchronization uses, forestry, etc., S-band becomes very beneficial and S-band signals are less affected by ionospheric errors than the L-band signals. They exhibit reduced phase noise and multipath. Considering that ionospheric effects dominate the total error budget, for single-frequency users, this can bring significant accuracy gain. From the simulation results of PSD, histograms and performance of acquisition and hypothesis testing, it is observed that NavIC reception on S-band frequency is severely affected by Wi-Fi transmission. The major out-of-band interference effect generated from the Wi-Fi router on S-band signals of the NavIC receiver is reported here. These interfering signals present a threat to the NavIC receiver performance. To equip both the facilities in future cell phones, it will be a challenge to mitigate such kind of RFI.

1. Dovis, F., GNSS Interference Threats and Counter Measures, Artech House, 2015, pp. 22–38.
2. Jagiwala, D. D. *et al.*, Study of L5 band interferences on IRNSS. In Proceedings of GNSS User Meet, Bangalore, India, 2015, p. 45.
3. Baghel, S. K., Ingale, M. A. and Goyal, G., Coexistence possibilities of LTE with ISM technologies and GNSS. In IEEE National Conference on Communication, Bangalore, India, 2011, pp. 1–5.
4. Mateu, I. *et al.*, Exploration of possible GNSS signals in S-band. In Proceedings of the 22nd International Technical Meeting of the Satellite Division of the Institute of Navigation (ION GNSS 2009), Savannah, GA, pp. 1573–1587.
5. Soualle, F. *et al.*, Assessment on the use of S-band for combined navigation and communication. In Proceedings of the 24th International Technical Meeting of the Satellite Division of the Institute of Navigation (ION GNSS 2011), September 2011, pp. 1219–1223.
6. Landry, R. J., and Renard, A., Analysis of potential interference sources and assessment of present solutions for GPS/GNSS receivers. In 4th Saint Petersburg International Conference on Integrated Navigation Systems, 1997, pp. 1–13.
7. Marti, L. and van Graas, F., Bias detection and its confidence assessment in global positioning system signals. In IEEE Aerospace Conference, Big Sky, MT, USA, 2004, 1418–1431.
8. Balaei, A. and Dempster, A., A statistical inference technique for GPS interference detection. *IEEE Trans. Aerosp. Electron. Syst.*, 2009, **45**(4), 1499–1511.
9. Tani, A. and Fantacci, R., Performance evaluation of a precorrelation interference detection algorithm for the GNSS based on non-parametrical spectral estimation. *IEEE Syst. J.*, 2008, **2**(1), 20–26.
10. Peck, R., Olsen, C. and Devore, J. L., *Introduction to Statistics and Data Analysis*, Cengage Learning, 2015, pp. 577–683.
11. IRNSS signal in space ICD August 2017, ISRO-ISAC V1.1; http://www.isro.gov.in/irnss-programme/
12. Desai, M. V., Jagiwala, D. and Shah, S. N., Impact of dilution of precision for position computation in Indian Regional Navigation Satellite System. In International Conference on Advances in Computing, Communications and Informatics (ICACCI), 2016, pp. 980–986.
13. Fadaei, N., Detection, characterization and mitigation of GNSS jamming interference using pre-correlation methods. Ph D dissertation, University of Calgary, Canada, 2016, p. 48.
14. Isoz, O., Interference detection and localization in the GPS L1 frequency band. Ph D dissertation, Lulea University of Technology, Sweden, 2012, pp. 11–12.

ACKNOWLEDGEMENTS. We thank Shri Tapan Mishra, Director, Space Applications Centre (SAC), ISRO, Ahmedabad, and Shri Atul Shukla, Shri Yagnesh Patel and Shri P. Akhileshwar Reddy (Scientists, SAC, ISRO) for their guidance.

Received 9 November 2017; revised accepted 6 February 2018

doi: 10.18520/cs/v114/i11/2273-2280